Effect of Submicron-Carbon-Containing MgO-C Refractories on Carbon Pickup of Ultra-Low Carbon Steel

Y. Liu[1, 2], L. Wang[2], G. Li[*1, 2, 3], Z. Zhang[2], X. Xu[1], Y. Li[1], J. Chen[1]

[1]The State Key Laboratory of Refractories and Metallurgy, Wuhan University
of Science and Technology, Wuhan 430081, China
[2]Key Laboratory for Ferrous Metallurgy and Resources Utilization of Ministry of Education,
Wuhan University of Science and Technology, Wuhan 430081, China
[3]Collaborative Innovation Center of Steel Technology, University of
Science and Technology Beijing, Beijing, 100083, China

Abstract

To reduce the carbon pickup of ultralow-carbon steel, the interaction between liquid steel and MgO-C refractories containing submicron carbon at 1600 °C was studied under laboratory conditions and compared with interaction of liquid steel with conventional MgO-C refractories containing flaky graphite. The results show that the carbon pickup in steel is provided by the spalling refractories, the penetration layer and the reaction of Al in steel with CO, which is generated from the reaction between MgO and C in refractories. The carbon supplied by spalling refractories might play a dominant role in the carbon pickup of steel. The reaction between Al in steel and CO is not the main cause of carbon pickup. In the test with conventional MgO-C refractories, carbon pickup became more severe with increasing content of flaky graphite. In the test with MgO-C refractories containing submicron carbon, the carbon pickup decreased with increasing submicron-carbon content, which is attributed to the thinner penetration layer and better spalling resistance. The application of MgO-C refractories containing submicron carbon could be favourable for the manufacture of ultralow-carbon steel with high cleanliness.

Keywords: Submicron carbon, MgO-C refractories, carbon pickup, penetration, spalling resistance

I. Introduction

MgO-C refractories are applied extensively in the steelmaking industry, for example for lining oxygen converters, arc furnaces and ladles in contact with liquid steel at elevated temperature during smelting processes. The introduction of graphite increases their thermal conductivity, which influences their thermal shock resistance and nonwetting behaviour in respect of slag, enhancing their slag corrosion resistance[1–4]. These enhanced properties are essential for their application in the steelmaking industry[5, 6]. However, a high carbon content in MgO-C refractories is detrimental to the production of high-quality ultralowcarbon steel because the carbon-bearing refractories can play a role as a carbon source[7, 8] and lead to more wetting between the liquid iron and refractories on account of the presence of carbon[9, 10], resulting in carbon pickup by the liquid steel. The interaction between conventional MgO-C refractories and molten steel has been well studied[11–15]. This interaction mainly includes two reactions as follows: 1) The reduction of MgO by carbon[11–14] 2) The oxidation of aluminium dissolved in steel by carbon monoxide formed at the interface[8, 15]. With the development of metallurgical technology, low-carbon refractories are es-

sential for the production of high-quality ultralow carbon steel. Furthermore, high-carbon refractories suffer from two major drawbacks, that is low mechanical strength and poor oxidation resistance[16]. So extensive research has been focused on low-carbon refractories[16–18], concentrating on the thermomechanical properties of these materials.

To further reduce the carbon content of MgO-C refractories while ensuring that the valuable properties of refractories do not deteriorate, nano-carbon is used as a carbon source in MgO-C refractories[19–24]. MgO-C refractories containing 1.5 % nano-carbon exhibit thermal spalling resistance equivalent to that of conventional refractories containing 18 % graphite[21]. Some studies indicate that nano-carbon-containing MgO-C refractories exhibit improved spalling resistance. The main reasons are that the nano-carbon suppresses the sintering of MgO and the mechanical properties are improved with increasing nano-carbon content[22, 23]. MgO-rimmed MgO-C bricks with less than 5 % carbon processed by applying a nanostructured matrix exhibit better thermal shock resistance and oxidation resistance than conventional bricks, while their corrosion resistance is almost on the same level[24]. Currently, the application of nano-carbon in refractories is associated with two main problems: 1) It is difficult to ensure the uniform distribution of the nano-carbon in refrac-

* Corresponding author: liguangqiang@wust.edu.cn

tories and 2) Nano-carbon is expensive[2]. To the authors' best knowledge, few of researches focus on the effect of submicron-carbon-containing MgO-C refractories on the carbon pickup of ultralow-carbon steel.

Because of these factors, the authors were motivated to undertake experiments in order to explore the underlying mechanism of the carbon pickup of ultralow-carbon steel during contact with submicron-carbon-containing MgO-C refractories. The interaction between submicron-carbon-containing MgO-C refractories and liquid steel and the properties of the refractories were studied and also compared with conventional refractories containing flaky graphite. This work was designed to provide fundamental knowledge for the selection of MgO-C refractories for the production of clean ultralow-carbon steel.

II. Experimental

(1) Materials preparation

Industrial pure iron was used as the ultralow-carbon steel in the experiment. The chemical composition of the ultralow-carbon steel studied is shown in Table 1. Two types of MgO-C refractories with different carbon sources, denoted TC and TN, were investigated. The composition of the MgO-C refractories used in the experiment is shown in Table 2. The submicron-carbon content was defined as 1 wt%, 2 wt% and 3 wt% because (1) It is difficult to ensure a uniform distribution of excessive submicron-carbon in the matrix, (2) The price of submicron-carbon is relatively high and excessive use of submicron-carbon in refractories is not practical and (3) One purpose of the present study is to reduce the carbon content in refractories. The raw materials were fused magnesia aggregate (1 – 3 mm and 0 – 1 mm, 97.37 wt% MgO, 0.24 wt% Al_2O_3, 0.90 wt% SiO_2, and 0.97 wt% CaO, Dashiqiao, China), fused magnesia powder (< 88 μm, 98.5 wt% MgO, Dashiqiao, China), flaky graphite (< 74 μm, 97.5 wt% fixed carbon, Qingdao, China), metallic Al powder (< 88 μm, 98 wt% Al, Xinxiang, China), boron carbide (< 44 μm, 99.9 wt% B_4C, Shanghai, China) and submicron carbon black N990 (100 – 700 nm, 99.5 wt% fixed carbon, SSA (10 m²/g), Wuhan, China). Additionally, thermosetting phenolic resin (liquid, 36 wt% fixed carbon, Zibo, China) was used as a binder. In addition to the aggregate, the powders were pre-mixed for 2 h. The fused magnesia aggregate and phenolic resin were then added and the powders were further mixed for 30 min in a mixer with a rotating speed of 80 – 100 rpm. The mixture was kneaded, before specimens measuring Φ 36 mm × 36 mm were prepared by means of cold pressing at 150 MPa and then curing at 200 °C for 24 h. Apparent porosity (AP) and bulk density (BD) were measured in accordance with the Chinese standard GB/T: 2997 – 2000. Cold crushing strength (CCS) was determined in accordance with the Chinese standard GB/T: 5072 – 2008.

(2) Interaction between MgO-C refractories and steel

The MgO-C refractories specimens were machined to a hollow cylinder with an inner diameter of 14 mm, an outer diameter of 36 mm and a height of 36 mm. Then the hollow cylinder and around 300 g ultralow-carbon steel were charged into an alumina crucible (ID = 42 mm), the steel being above the cylinder. In order to prevent leakage of liquid steel, the alumina crucible was placed into a graphite crucible. Six tests were performed in a vertical tube furnace with $LaCrO_3$ bars as heating elements at 1600 °C under Ar atmosphere (99.999 vol% purity) with a flow rate of 3.4 × 10^{-6} m^{-3}/s. The experimental apparatus is shown in Fig. 1. After 60-min holding time, a steel specimen was taken by means of suction through a quartz tube (ID = 4 mm) from the molten steel. Because the volume of the molten steel is not large, the sample taken is representative for composition analysis. Subsequently, the furnace was cooled to room temperature. The carbon content of the steel was determined with a carbon sulphur analyser by means of inert gas fusion-infrared absorptiometry. To measure the Al and Mg content in the steel, about 0.2 g steel was dissolved in a HCl solution (HCl : H_2O = 1.1). After filtration, the solution was analysed by means of ICP-AES. The interface between the MgO-C refractories and steel was analysed with a SEM (Nova 400 Nano) equipped with EDS (Le350 PentaFETx-3).

Table 1: Chemical composition of industrial pure iron used in the experiment (wt%).

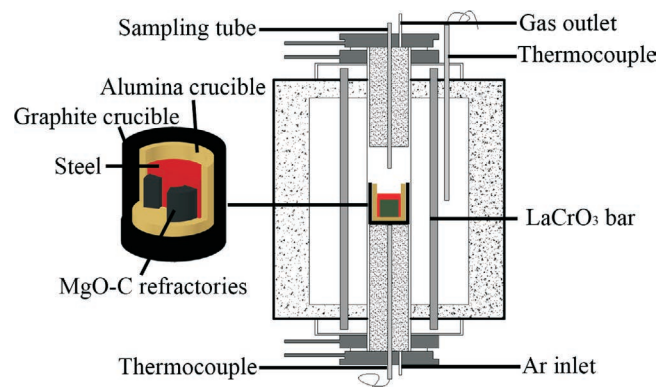| C	Si	Mn	P	S	Al	Mg
0.0038	0.03	0.06	0.015	0.005	<0.007	<0.003

Fig. 1: Experimental set-up.

III. Results and Discussion

(1) The changes of AP, BD and CCS of refractories containing varying carbon sources

Fig. 2 shows the change of the AP with the carbon content of MgO-C refractories with varying carbon sources. It can be seen that the AP of traditional MgO-C refractories increases with increasing carbon content, whereas the opposite trend is found in MgO-C refractories containing submicron carbon. It is well known that the AP of refractories is dominated by the microstructure of the raw materials. Fig. 3 shows micrographs of the MgO with the size of < 88 μm and 1 – 3 mm. It indicates that many pores and voids exist in the coarse MgO particles. Fig. 4

Table 2: Batch composition (wt%).

Raw materials	TC-1	TC-2	TC-3	TN-1	TN-2	TN-3
MgO (1–3 mm)	40	40	40	40	40	40
MgO (0–1 mm)	30	30	30	30	30	30
MgO (<88 μm)	25.6	23.5	18.4	26	25	24
Flaky graphite	1.4	3.5	8.6	0	0	0
Submicron carbon black (N990)	0	0	0	1	2	3
Metallic Al powder	2.5	2.5	2.5	2.5	2.5	2.5
B_4C powder	0.5	0.5	0.5	0.5	0.5	0.5
Liquid resin	4	4	4	4	4	4

shows micrographs of flaky graphite and submicron carbon N990. It can be seen that the size of the flaky graphite is large, which leads to an uneven distribution (Fig. 4a, 4b). The submicron carbon N990 is smaller in size than flaky graphite, leading to a more even distribution (Figs. 4c, 4d). For traditional refractories, the size of the flaky graphite is too large to effectively fill the voids and pores between the coarse, medium, and fine MgO particles. Moreover, the flaky graphite remains free to form new pores. So the AP of traditional MgO-C refractories increases with the increase in carbon content. For the refractories containing submicron carbon, the carbon source has a small size, which can fill voids and pores between the coarse, medium, and fine MgO particles. As a result, the AP of refractories containing submicron carbon shows a decreasing trend with increasing carbon content.
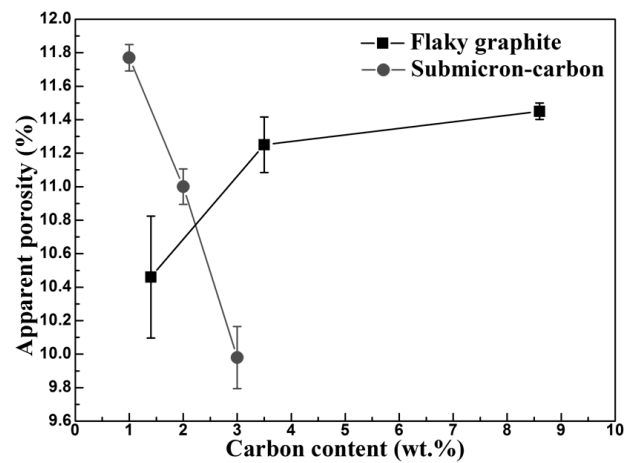

Fig. 2: Variation of apparent porosity with the carbon content of MgO-C refractories with varying carbon sources.
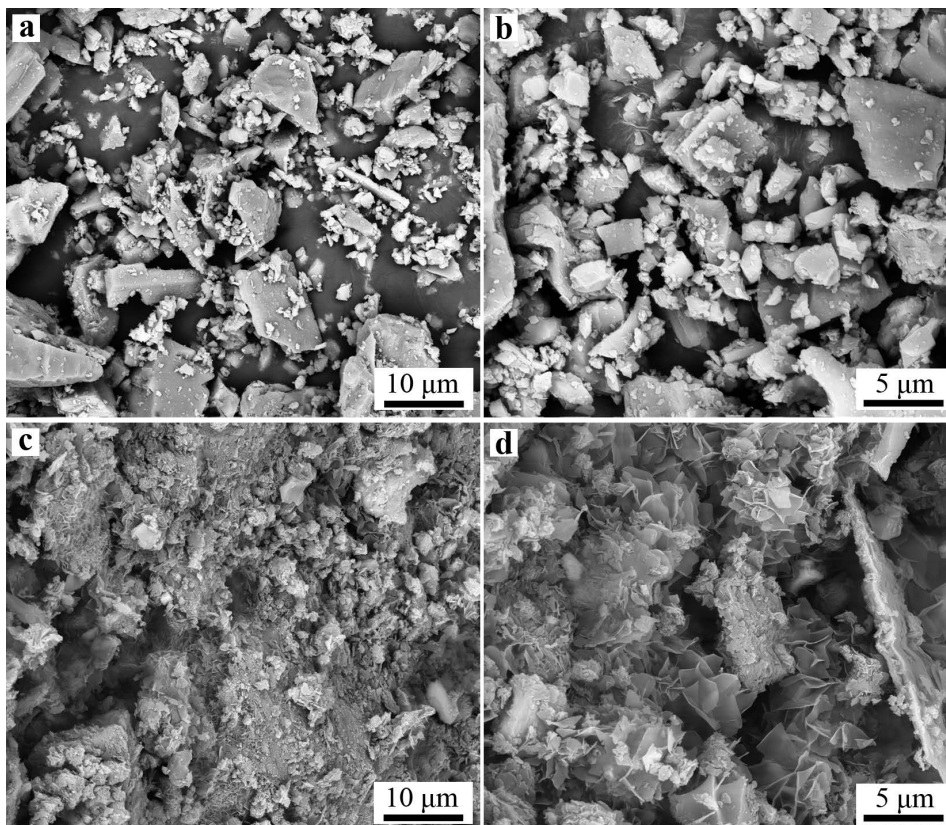

Fig. 3: Micrographs of MgO with the size of (a, b) <88 μm and (c, d) 1–3 mm.
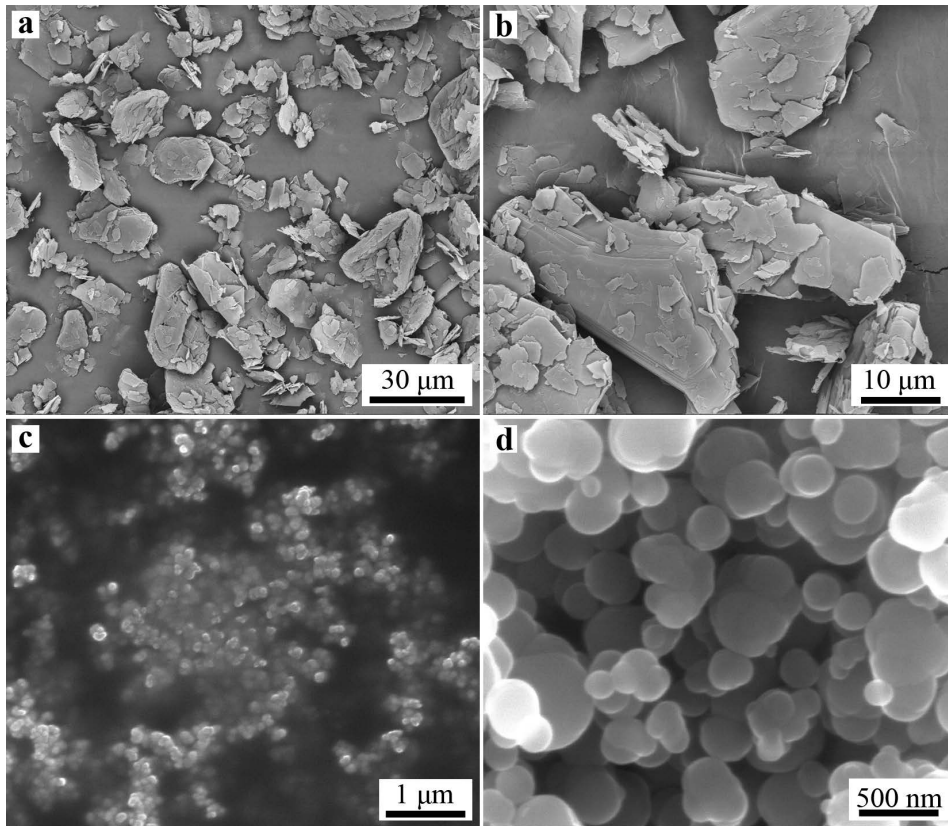
Fig. 4: Micrographs of (a, b) flaky graphite and (c, d) submicron carbon black N990.

Fig. 5 shows the change in BD with the carbon content of MgO-C refractories with varying carbon sources. The change trends support exactly the changes in AP. The BD of traditional MgO-C refractories decreases with the increase in carbon content because the AP increases and the density of the carbon is lower than that of the MgO. The BD of refractories containing submicron carbon shows the expected increasing trend owing to the decrease in AP.
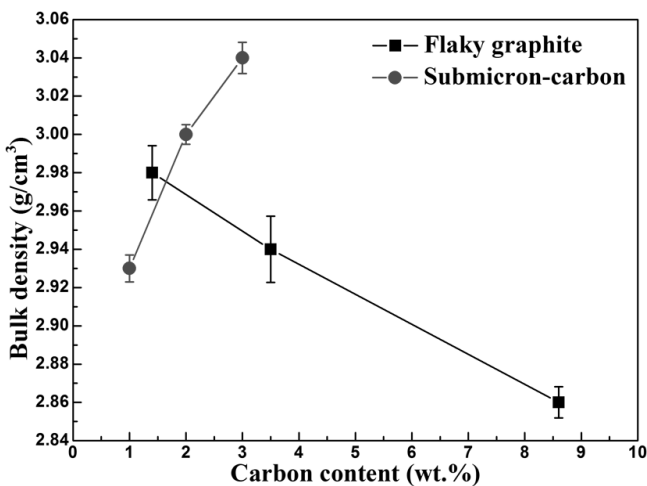
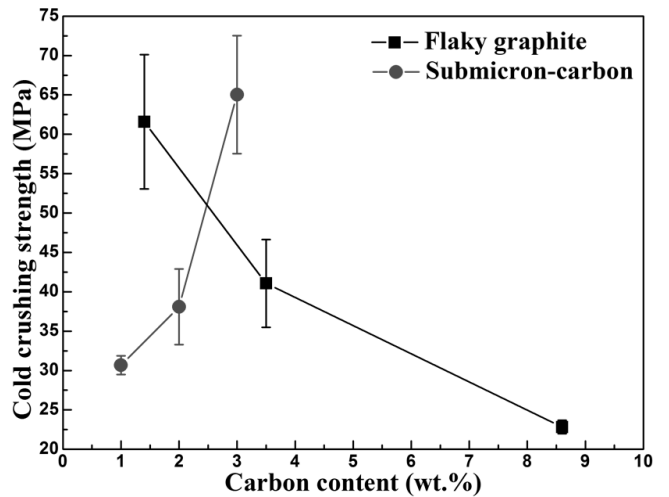fractories containing submicron carbon. This implies that a denser structure contributes to the improvement in CCS.

Fig. 6: Variation of cold crushing strength with the carbon content of MgO-C refractories with varying carbon sources.

Fig. 5: Variation of bulk density with the carbon content of MgO-C refractories with varying carbon sources.

Fig. 6 shows the change in the CCS with the carbon content of MgO-C refractories with varying carbon sources. The change in the CCS shows an opposite trend to that of AP, namely, CCS of traditional refractories decreases with the increase in carbon content, whereas it increases in re-

(2) Interaction between refractories and steel

Fig. 7 shows the microstructure of the interface between steel and MgO-C refractories with distinct carbon sources and contents. After the interaction between refractories and steel, a penetration layer exists at the interface between the steel and MgO-C refractories. Fig. 8 shows the change in the penetration layer thickness in MgO-C refractories with different carbon sources and contents. It indicates that penetration layer thickness increases from 30.8 μm to 38.5 μm and 42.3 μm with the flaky graphite content
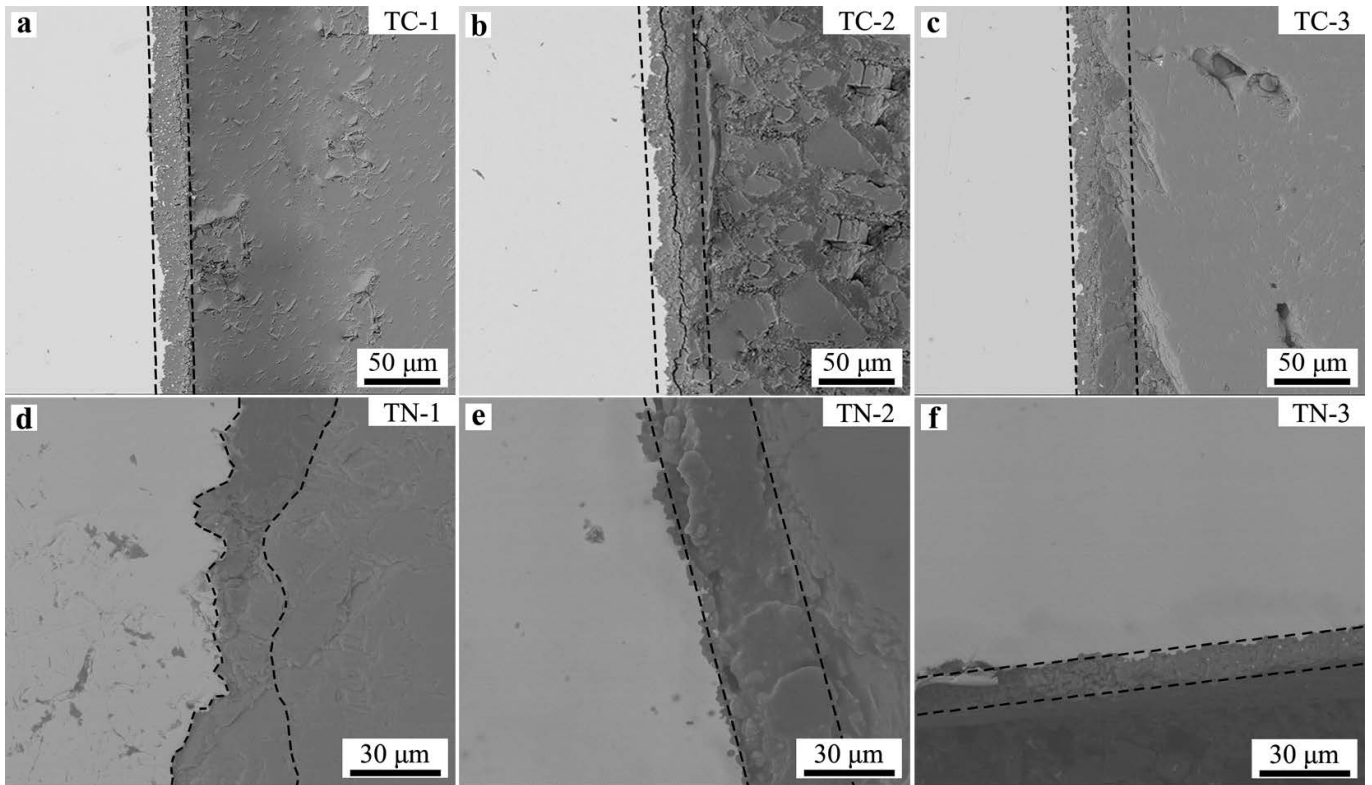
Fig. 7: Micrograph of the interface between the steel and MgO-C refractories with distinct carbon sources and contents: (a-c) TC and (d-f) TN9.

increasing from 1.4 wt% to 3.5 wt% and 8.6 wt% in the case of traditional refractories (Figs. 7a-c and 8), whereas, in the test with MgO-C refractories containing submicron carbon, the penetration layer thickness decreases with the increase in submicron-carbon content (Figs. 7d-f and 8). Fig. 9 shows a high-magnification SEM image and element mappings of the interface between refractories containing flaky graphite and steel. It indicates that liquid steel infiltrates into the penetration layer, and it is observed that carbon concentration in the penetration layer is lower. Inclusions exist in the vicinity of the interface and have the same composition as the refractories, implying that they are the results of erosion of the refractories.
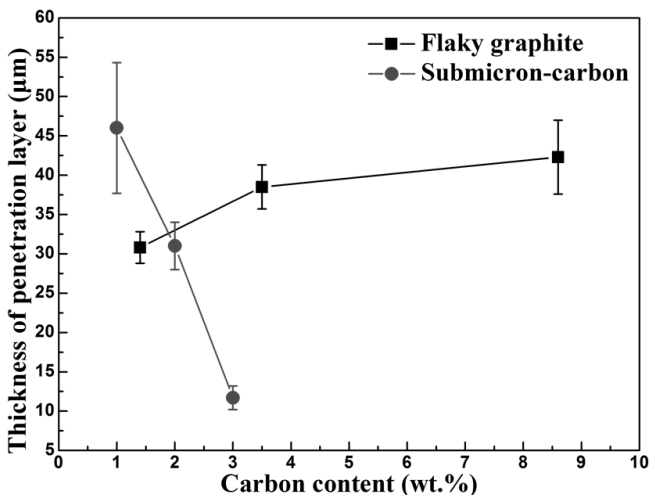

Fig. 8: Change of the penetration layer thickness in the MgO-C refractories with different carbon sources and contents.

The liquid steel flows into the pores of the refractories, resulting in steel penetration[25]. The pores in the refractories at 1600 °C holding temperature consist of pores at room temperature and new pores formed by carbon oxidation during heating. It is well known that carbon in MgO-C refractories can be oxidized in two ways: (1) Direct oxidization, mainly occurs under 1400 °C as a result of reaction (1); (2) Indirect oxidization, mainly occurs above 1400 °C as a result of reaction (2) as follows[5, 18, 26]:

$$2C(s)+O_2(g)=2CO(g) \qquad (1)$$

$$C(s)+MgO(s)=Mg(g)+CO(g) \qquad (2)$$
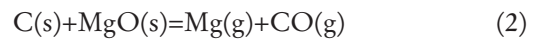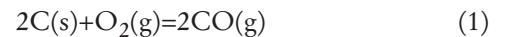
The present experiments were performed in a high-purity Ar atmosphere. The carbon of refractories can only be oxidized by the oxygen from the pores of refractories. So, the higher the AP is, the more severe the carbon oxidation is. Carbon oxidation further increases the porosity as a result of the formation of CO during heating from room temperature to 1600 °C, then molten steel flows into the pores, resulting in more severe steel penetration. In the case of traditional refractories, the AP shows an increasing trend with increasing flaky graphite content, so more severe steel penetration would occur with an increase in flaky graphite. In contrast, in the test with refractories containing submicron carbon, the AP decreases with the increase of submicron-carbon content, as a result, poor steel penetration would occur with the increase in carbon content. It can be seen from Figs. 2 and 8 that higher AP must lead to larger penetration layer thickness.
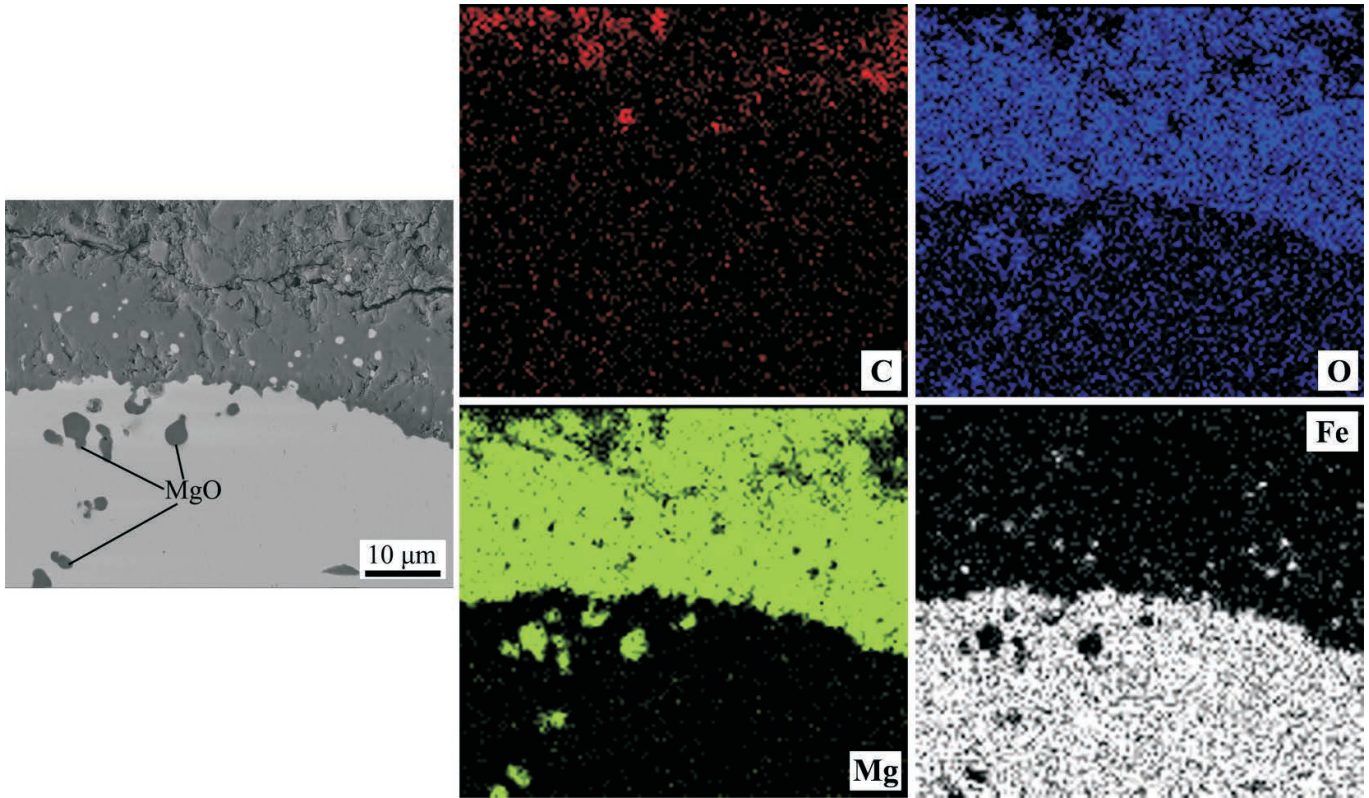
Fig. 9: SEM image and element mappings of the interface between MgO-C refractories and steel.

Fig. 10a shows the pickup of carbon content in steel with the carbon content of MgO-C refractories. It indicates that after 60 min holding, the carbon content in steel increases in all the refractories tests. The carbon pickup of steel becomes more severe with the increasing flaky graphite content of traditional refractories. However, in refractories containing submicron carbon, the carbon pickup of steel is reduced with the increase in submicron-carbon content. Fig. 10b shows the variations of [Mg] and [Al] contents in steel with the carbon content of MgO-C refractories. The varying trends are consistent with the carbon content in the steel. The carbon pickup mainly occurs in two forms: (I) Carbon from the refractories is dissolved in molten steel; (II) Carbon

reacts with MgO in refractories to form CO by reaction (2)[11–14], then [Al] in the molten steel reacts with CO to increase the carbon content in the steel according to the following reaction (3) as follows[8, 15]:

$$2[Al]+3CO(g)=Al_2O_3(g)+3[C] \qquad (3)$$
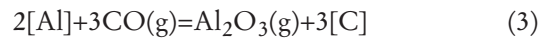
It is assumed that all the carbon in the penetration layer is dissolved into liquid steel. The carbon supplied by the penetration layer to liquid steel can be roughly estimated according to the penetration layer volume (V) and carbon content per unit volume (D) in refractory materials. Table 3 shows the fixed carbon content per unit volume in refractory materials. Fig. 11 shows the sketch for volume calculation of the penetration layer.
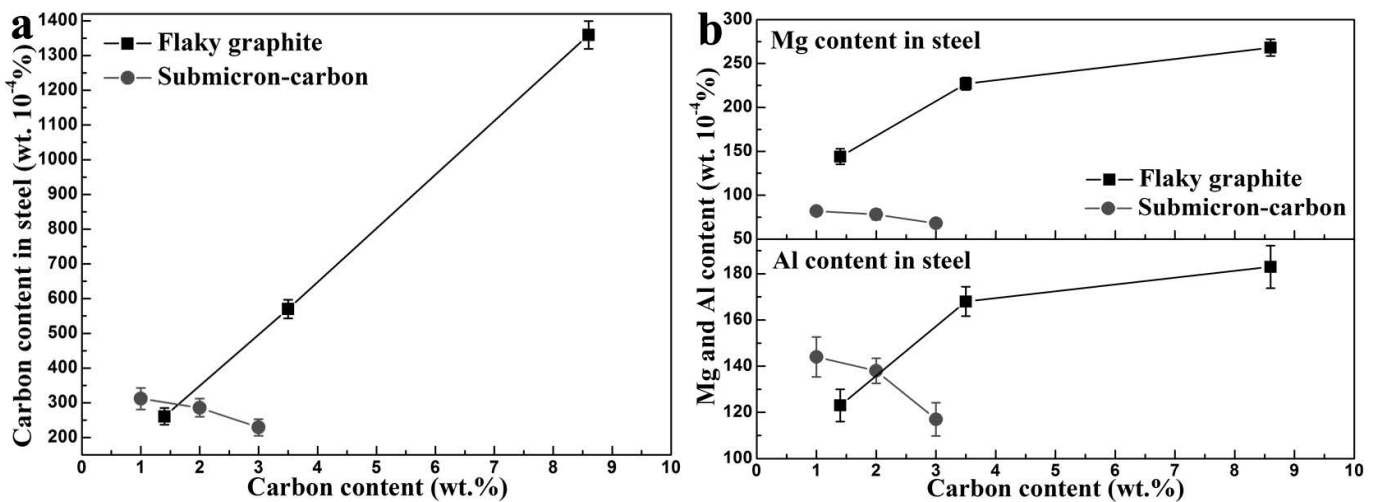

Fig. 10: Variation of (a) carbon, (b) Mg and Al contents in steel with the carbon contents of MgO-C refractories with varying carbon sources.

Table 3: The fixed carbon content per unit volume in refractory materials (10^{-3} g/cm^3).

Refractories	TC-1	TC-2	TC-3	TN-1	TN-2	TN-3
Carbon content	85	143	279	72	103	133

The volume can be calculated with Eq. (4) as follows:

$$V \approx 2\pi \cdot (R^2 - r^2) \cdot s + 2\pi \cdot (R + r) \cdot s \cdot h \qquad (4)$$

where R, r, s and h are the outer diameter, inner diameter, the penetration layer width and height of the refractories, respectively. The carbon supplied by the penetration layer to the liquid steel (C_p) can be roughly calculated with the following Eq. (5):

$$C_p \approx \frac{D \cdot V}{m_s} \qquad (5)$$

where m_s is the steel mass, 300 g. The total amount of carbon pickup in molten steel (C_t) was calculated with Eq. (6):

$$C_t = C - C_o \qquad (6)$$

where C is the carbon content of steel after test (weight 10exp-4 %), C_o is the original carbon content in steel. According to Eq. (4 – 6) and the data in Table 3, the carbon supplied by the refractories was calculated. Fig. 12 shows the carbon supplied by the refractories with different carbon sources and contents. It can be seen that the carbon supplied by the penetration layer to the liquid steel (C_p) is far below the total amount of carbon pickup, which consists of carbon supplied by penetration layer (C_p), the carbon from the spalling refractories and carbon supplied by reaction (2, 3) (indicated as C_r). Quantitative calculation of the carbon from the spalling refractories and the carbon supplied by reaction (2, 3) could not be realized. But qualitative analysis can be performed. The Al and Mg contents in steel are low before interaction, the Al and Mg pickup in steel is only attributed to the spalling refractories. It should be noted that Al content determined is the acid-soluble aluminium, which does not contain the Al$_2$O$_3$ inclusions, whereas the MgO inclusions can be dissolved in the acid. The Mg content determined contains the Mg dissolved in the steel and the Mg from MgO inclusions. The Mg content dissolved in the steel is low owing to the high vapour pressure of Mg. The excessive Mg content in the steel should result from the MgO inclusions in the steel. It can be seen from Fig. 10b that the Al and C contents of steel in the test of refractories with 1 wt% submicron carbon are higher than those in traditional refractories with 1.4 wt% submicron carbon, indicating that the more severe abscission occurs in the refractories with 1 wt% submicron carbon, whereas the lower Mg content is observed in the test on refractories with 1 wt% submicron carbon owing to the flotation of MgO inclusions. In the test on refractories containing submicron carbon, the C, Mg and Al contents in the steel decrease with the increasing submicron-carbon content, but the opposite trend is found in the test on traditional refractories. The previous studies have confirmed that addition of a small-size carbon source can improve

spalling resistance[22, 23, 27]. Compared with the refractories containing submicron carbon, more refractory particles from traditional refractories would drop into the molten steel. As a result, the C, Mg and Al contents in the steel show an increasing trend with increasing flaky graphite content in the test on traditional refractories (Fig. 10b). In general, the amount of carbon provided by reaction (2, 3) should be increased with more carbon in the refractories. The amount of carbon supplied by reaction (2, 3) should be small in the present experiment, because the carbon content in the steel shows a decreasing trend with the increasing submicron carbon content in the test on refractories containing submicron carbon. The addition of submicron carbon to the MgO-C refractories contributes to the production of ultralow-carbon steel with high cleanliness owing to the lower AP and better spalling resistance. The better spalling resistance can reduce the large inclusions in the steel.
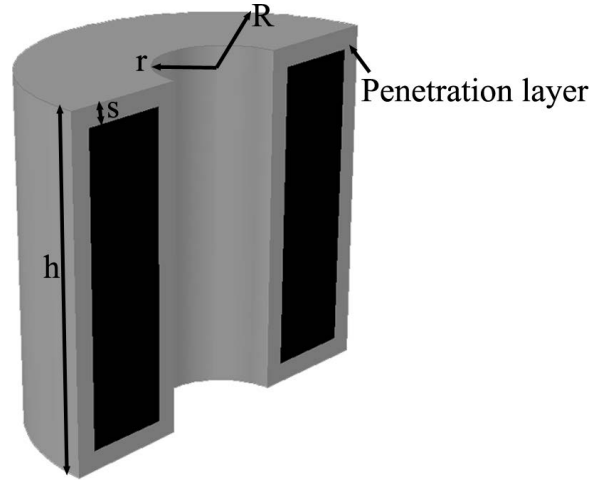

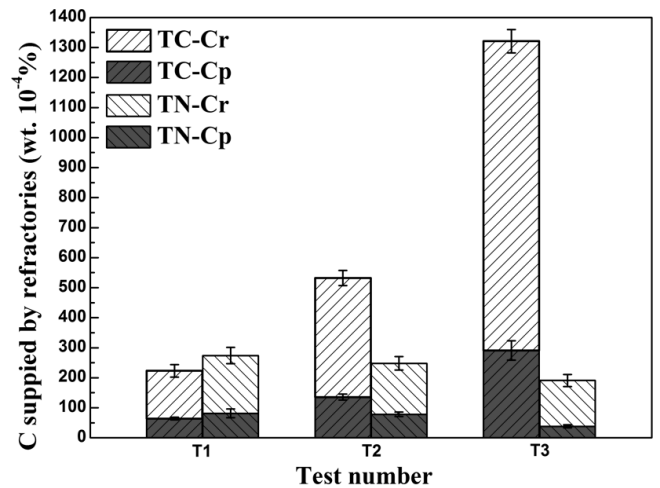**Fig. 11:** Sketch for volume calculation of penetration layer of refractories.

Fig. 12: The carbon supplied by the MgO-C refractories.

IV. Conclusions

The following conclusions can be drawn from the present study:

(1) With the addition of submicron carbon to MgO-C refractories, the apparent porosity decreases while bulk density and cold crushing strength increase. In convention-

al refractories with flaky graphite, the opposite trends are observed with the increase of the flaky graphite content in the refractories.

(2) The penetration layer thickness is dominated by the apparent porosity. A lower apparent porosity can reduce penetration layer thickness. The carbon pickup in steel is provided by the spalling refractories, the penetration layer and the reaction of Al and CO generated from the reaction of the MgO and C in refractories. The penetration layer provides only a small amount of carbon. The carbon supplied by spalling refractories might playing a dominant role in the carbon pickup of steel.

(3) The carbon pickup becomes more severe with increasing flaky graphite content in the test on conventional MgO-C refractories. In the test on MgO-C refractories containing submicron carbon, the carbon pickup decreases with the increase in submicron-carbon content, which is attributed to the lower penetration layer width and better spalling resistance. The MgO-C refractories containing submicron carbon could be promising refractories for the manufacture of ultralow carbon steel with high cleanliness.

Acknowledgements

References

[1] Cooper, C.F., Alexander, I.C., Hampson, C.J.: The role of graphite in the thermal shock resistance of refractories, *Br. Ceram. Trans. J.*, **84**, 57–62, (1985).

[2] Liang, F., Li, N., Liu, B., He, Z.: Processing and characterization of multi-walled carbon nanotubes containing alumina-carbon refractories prepared by nanocomposite powder technology, *Metall. Mater. Trans. B*, **47**, 1661–1668, (2016).

[3] Benedetti, B.D.E.: The resin union magnesium carbon brick bears corrosiveness, *Br. Ceram. Trans. J.*, **3**, 55–57, (1989).

[4] Chen, J., Li, N., Yan, W.: Influence of Ti_3AlC_2 on corrosion resistance and microstructure of Al_2O_3-Ti_3AlC_2-C refractories in contact with ladle slag, *J. Eur. Ceram. Soc.*, **36**, 1505–1511, (2016).

[5] Faghihi-Sani, M.A., Yamaguchi, A.: Oxidation kinetics of MgO-C refractory bricks, *Ceram. Int.*, **28**, 835–839, (2002).

[6] Sasai, K., Mizukami, Y.: Reaction rate between alumina graphite immersion nozzle and low carbon steel, *ISIJ Int.*, **35**, 26–33, (1995).

[7] Ruan, G.Z., Li, N.: Carbon pickup of interstitial free steel from Al_2O_3-C refractories, *Ironmak. Steelmak.*, **31**, 342–344, (2004).

[8] Jansson, S., Brabie, V., Jönsson, P.: Magnesia-carbon refractory dissolution in al killed low carbon steel, *Ironmak. Steelmak.*, **33**, 389–397, (2006).

[9] Zhao, L., Sahajwalla, V.: Interfacial phenomena during wetting of graphite/alumina mixtures by liquid iron, *ISIJ Int.*, **43**, 1–6, (2003).

[10] Lee, J., Tazuke, A., Tanaka, T., Park, J.H.: Estimation of sulfur segregation at the interface between molten iron and graphite substrate from wetting experiments, *Met. Mater. Int.*, **15**, 501–505, (2009).

[11] Pickering, G.D., Batchelor, J.D.: Carbon-MgO reactions in BOF refractories, *Am. Ceram. Soc. Bull.*, **50**, 611–614, (1971).

[12] Robinson, P.C.: Some observation on unused and used refractories from oxygen steelmaking vessels, *Refract. J.*, **42**, 218–222, (1966).

[13] Kim, S.M., Lu, W.K.: Kinetics and mechanism of the formation of dense MgO layer in pitch-bearing magnesite brick during service, *Metall. Trans. B*, **9**, 353–364, (1978).

[14] Watanabe, A., Takahashi, H., Nakatani, F.: Mechanism of dense magnesia layer formation near the surface of magnesia-carbon brick, *J. Am. Ceram. Soc.*, **69**, 213–214, (1986).

[15] Brabie, V.: A study on the mechanism of reaction between refractory materials and aluminium deoxidised molten steel, *Steel Res. Int.*, **68**, 54–60, (1997).

[16] Zhu, T., Li, Y., Sang, S., Jin, S., Wang, H.: Formation of hollow MgO–rich spinel whiskers in low carbon MgO-C refractories with al additives, *J. Eur. Ceram. Soc.*, **34**, 4425–4432, (2014).

[17] Hashemi, B., Nemati, Z.A., Faghihi-Sani, M.A.: Effects of resin and graphite content on density and oxidation behavior of MgO-C refractory bricks, *Ceram. Int.*, **32**, 313–319, (2006).

[18] Gokce, A.S., Gurcan, C., Ozgen, S., Aydin, S.: The effect of antioxidants on the oxidation behaviour of magnesia-carbon refractory bricks, *Ceram. Int.*, **34**, 323–330, (2008).

[19] Bag, M., Adak, S., Sarkar, R.: Study on low carbon containing MgO-C refractory: Use of nano carbon, *Ceram. Int.*, **38**, 2339–2346, (2012).

[20] Bag, M., Adak, S., Sarkar, R.: Nano carbon containing MgO-C refractory: Effect of graphite content, *Ceram. Int.*, **38**, 4909–4914, (2012).

[21] Ochiai, T.: Development of refractories by applying nanotechnology, *Refractories* (Tokyo), **56**, 152–159, (2004).

[22] Xuejun, Y., Zheming, Q., Liangquan, H.: The influence of nanometer carbon black on the mechanical properties of phenolic resin, *Process. Aircraft. Mater.*, **33**, 34–38, (2003).

[23] Xianhui, L., Chifei, W.: The optimization of characterization and preparation on nanometer carbon blacks, *Process. Technol. Nano. Mater.*, **2**, 47–49, (2005).

[24] Takanaga, S., Fujiwara, Y., Hatta, M.: Nano–Tech. refractories 3: Development of MgO-rimmed MgO-C brick. In: Proceedings of the 9th UNITCER-2005. Orlando, FL, USA, 2005.

[25] Wei, Y., Li, N., Ke, C.: Effect of silicon carbide on reactions between molten steel and fused magnesia-silicon carbide composite refractory, *Am. Ceram. Soc. Bull.*, **86**, 9201–9205, (2007).

[26] Li, X., Rigaud, M., Palco, S.: Oxidation kinetics of graphite phase in magnesia-carbon refractories, *J. Am. Ceram. Soc.*, **78**, 965–971, (1995).

[27] Xiaoqiang, S., Lin, L, Xiaoyan, P.: Effects of nanometer carbon black on the mechanical properties and thermal shock resistance of MgO-C bricks, in chinese, *China Metallurgy*, **6**, 17–20, (2015).